

november 2019

# Seismic Q-filter models applied to the Riccati equation

Knut Sørsdal

Norway, 2019

## Abstract

A theoretical study is made of an inversion technique of the Riccati type. This paper employs Q-models to introduce forward and inverse filtering of a seismic wave propagating in a visco-elastic solid. The solution of the Riccati equation with the Kelvin Voigt absorption model has been given by Nilsen and Gjevik. The linear solution of the wave equation introducing attenuation and dispersion has been studied by Wang. He used a modification of Kolsky's Q-model and applied it on a downward continuation algorithm. I have taken Nilsen and Gjevik's theory further with a general Q-model and a more elegant inversion.

## Introduction

At present there is a considerable interest in inversion techniques for seismic reflection data. The reason for this interest is the belief that these data carry information which is either unrevealed or lost by conventional data processing. Seismic inverse Q-filtering (IQF) is one sector of regular inversion technics. It employs a wave propagation reversal procedure that compensates for energy absorption and corrects wavelet distortion due to velocity dispersion. By compensating for amplitude attenuation with a model of the visco-elastic attenuation model type, seismic data can provide true relative-amplitude information for amplitude inversion and subsequent reservoir characterization. By correcting the phase distortion due to velocity dispersion, seismic data with enhanced vertical resolution can yield correct timings for lithological identification.

This article use an inversion method based on the Riccati-equation. An attempt with this inversion method was done by Gjevik et al. (1975) where some impedance models were introduced. In another article Nilsen and Gjevik (1978) presented the theory in a broader way and one absorption model was included. Their theory has been further developed by Sørdsal (1981) and was presented in two previous papers on Researchgate (Sørdsal (2018) and Sørdsal (2) (2018)).

Nilsen and Gjevik introduced an attenuation model of the Kelvin Voigt type and suggested to include inversion with absorption using the standard least square deconvolution method as part of the Riccati equation. As far as we know, Nilsen and Gjevik presented no calculations with absorption.

We will briefly recapitulate their theory by introducing a general absorption model in a forward modelling approach. From this general model we will end up with Q-models of which one will be used in modelling for the inversion. We also include the Kelvin Voigt model and the non-casual Futterman model but these models are not used in the inversion since they are non-causal. Finally, we do inverse Q-filtering on a simple impedance model. We calculate first with the LSQ-solution presented, and then with Gjevik's solution with IQF implemented. We got very similar solutions.

## Basics of modelling with absorption included

Inverse Q-filtering algorithms are mainly based on forward wave propagation migration type approach. Then the decay of the frequency content due to absorption can be inspected at each time sample. (Wang (2007).) Following Gjevik we can assume monochromatic plane-waves propagating along a vertical axis. Let  $P$  define the stress (pressure) and  $W$  the displacement. Density is  $\rho$ . Newton's second law gives:

$$\frac{dP}{dz} + \rho\omega^2 W = 0 \quad (1)$$

Correspondingly, a stress-strain relationship of the following form is assumed (Hook's law):

$$P = \rho v_r^2 Y \frac{dW}{dz} \quad (2)$$

In Eq.(2)  $v_r$  is the reference velocity which could be taken as the group velocity in case of dispersion. The function  $Y$  represents depth and frequency-dependent absorption.

In case of no damping,  $Y=1$  and Eq.(2) is simply Hookes law.

Combination of Eqs.(1) and (2.b) gives Helmholtz equation (assume constant density)

$$\frac{d^2 P}{dz^2} + k^2 P = 0, k = \frac{\omega}{v_r \sqrt{Y}} \quad (3)$$

To achieve a complex damping function we can follow Horton (1959) and introduce the notation

$$Y(\omega, \tau) = A(\omega, \tau) + iB(\omega, \tau) \quad (4)$$

In his paper, Horton gives examples of values of A and B for various absorption models that can be causal or non-causal. Since the wavenumber k is in focus, the following expression is now elaborated on

$$\frac{1}{\sqrt{Y}} = \frac{1}{\sqrt{A+iB}} = \frac{\sqrt{A-iB}}{\sqrt{A^2+B^2}} = \frac{(A^2+B^2)^{1/4} [\cos(u/2) - i \sin(u/2)]}{(A^2+B^2)^{1/2}} = \frac{[\cos(u/2) - i \sin(u/2)]}{(A^2+B^2)^{1/4}}$$

$$\tan(u) = \frac{B}{A} \quad (5)$$

Moreover, the following trigonometric relations are valid

$$\tan(u) = \frac{\sin(u)}{\cos(u)} = \frac{\sin(u)}{\sqrt{1-\sin^2(u)}} = \frac{\sqrt{1-\cos^2(u)}}{\cos(u)} = \frac{B}{A} \Rightarrow \quad (6)$$

$$\cos(u) = \frac{A}{\sqrt{A^2+B^2}}, \quad \sin(u) = \frac{B}{\sqrt{A^2+B^2}}$$

And also these

$$\cos(u/2) = \sqrt{\frac{1+\cos(u)}{2}}, \quad \sin(u/2) = \sqrt{\frac{1-\cos(u)}{2}} \quad (7)$$

Finally, combination of Eqs. (5)-(7) gives the result

$$k = \frac{\omega}{v_r \sqrt{Y}} = \frac{\omega}{v_r \sqrt{A+iB}} = \frac{\omega}{v_r} \left[ \frac{1}{\sqrt{A}} - \frac{i}{2} \frac{B}{A\sqrt{A}} \right] \quad (8)$$

Now we will compare the real and imaginary part of k for the Q-models. The theory for the different models are in appendix 1 and presented in Table 1. The real part can be related to the phase velocity and the imaginary part is the attenuation coefficient.

$$\text{Then we have: } k_{real} = \frac{\omega}{v_r} \frac{1}{\sqrt{A}} \quad \text{and} \quad k_{imag} = \frac{1}{2} \frac{\omega}{v_r} \frac{B}{A\sqrt{A}} \quad (9)$$

| Model                  | A   | B  |
|------------------------|---|--|
| 1 Kolsky - Wang        | $\left[\frac{\omega}{\omega_h}\right]^{2\gamma} \gamma = \frac{1}{\pi Q}$ | $\left[\frac{\omega}{\omega_h}\right]^{2\gamma} \frac{1}{Q}$ |
| 2 Futterman non-causal | 1   | $\frac{1}{Q}$  |
| 3 Kelvin Voigt         | 1   | $\omega \frac{q}{\rho v_r^2}$                                |
| 4 Causal Futterman     | $\left[1 + \frac{1}{\omega} H\left(\frac{\omega}{2Q}\right)\right]^{-2}$  | $(A_{Futt})^{3/2} \frac{1}{Q}$                               |

Table 1 Forward Q-filter models

Fig.1. shows  $\sqrt{A}$  (which gives us a hint about the dispersion) for Kolsky-Wang  $2\pi\omega_h=125$  Hz (blue graph) and  $2\pi\omega_h=500$  Hz (black). (Multiplying  $\sqrt{A}$  with the reference velocity  $v_r$  gives us the phase velocity). Red graph is causal Futterman. A small tuning frequency gives Wang a better fit to Futterman causal than a higher one. Wang choose the tuning frequency as the highest frequency of the model with the Nyquist frequency as the actual choice. Both Futterman non-causal and Kelvin Voigt have the same value  $A=1$  for all frequencies resulting in no dispersion. The attenuation coefficient shows that Futterman causal has smallest damping and smallest dispersion. Wang used Kolsky with highest tuning frequency (500 Hz). It has slightly more attenuation than the lower (125Hz) for the same value of  $Q=25$ . And also more dispersion (black dotted graph).

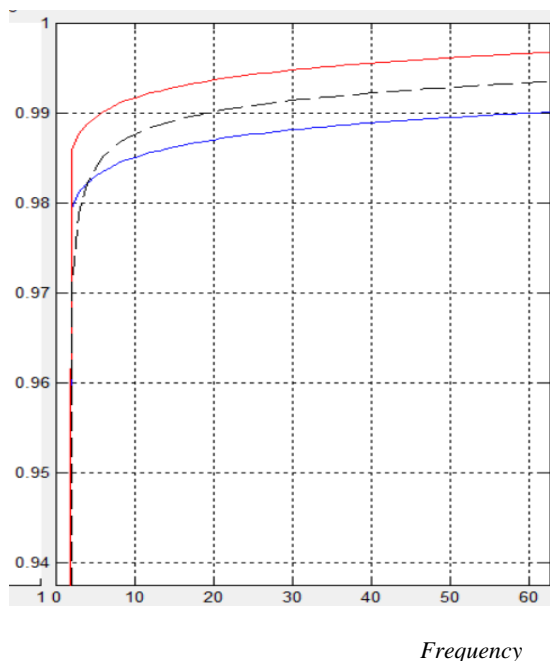


Fig.1. Comparing phase for Q-models

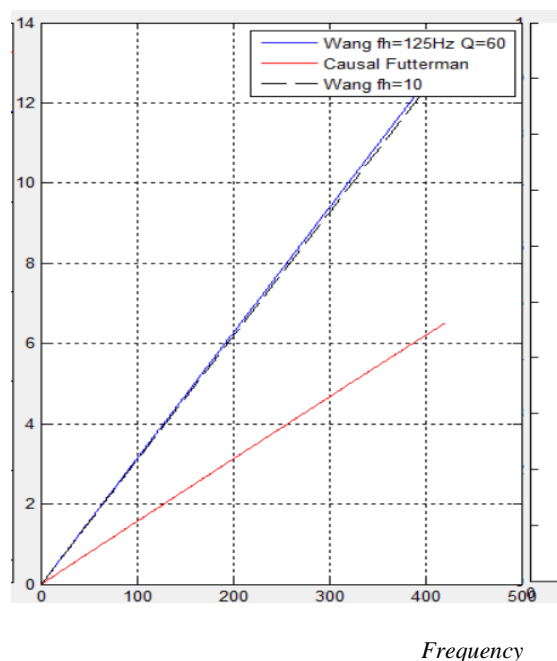


Fig.2. Comparing attenuation for Q-models

### Introducing the Riccati equation with absorption

The basic idea in a downward wave propagation migration approach is that the wavefield at the surface of the seismic earth model is extrapolated down to a depth  $z$ . The real part of  $k$  in Eq. (9) describes all dispersion effects during wave propagation and the imaginary part describes absorption.

From Nilsen and Gjevik (1978) we have the Riccati equation:

$$\frac{dK}{dz} = \frac{2i\omega}{v_r \sqrt{Y}} K - r(1 - K^2) \quad (10)$$

$K$  is the complex reflection coefficient and  $r$  is the depth-dependent 'reflectivity' per depth unity:

$$r(\tau) = \frac{1}{2\rho v_r} \frac{d(\rho v_r)}{d\tau} \quad (11)$$

Since vertically travelling waves are considered, the transformation from depth to two-way traveltime is straightforward

$$\tau = 2 \int_0^z \frac{dz}{v_r}, \Rightarrow d\tau = \frac{2}{v_r} dz \quad (12)$$

Which gives the travel time version of Eq.(10)

$$\frac{dK(\omega, \tau)}{d\tau} = \frac{i\omega}{\sqrt{Y(\omega, \tau)}} K(\omega, \tau) - r(\tau)(1 - K^2), r(\tau) = \frac{1}{2\rho v_r} \frac{d(\rho v_r)}{d\tau} \quad (13)$$

By noticing that

$\exp(-i\omega \int_0^\tau Y(\omega, \tau')^{-1/2} d\tau') \equiv \exp[-\phi(\omega, \tau)]$  is an integrating factor for this Riccati equation, it can be rewritten on the following form:

$$\frac{d}{d\tau} [K(\omega, \tau) \exp(-\phi(\omega, \tau))] = -r(\tau)(1 - K^2) \exp(-\phi(\omega, \tau)) \quad (14)$$

Where

$$\phi(\omega, \tau) = i\omega \int_0^\tau \frac{d\tau'}{\sqrt{Y(\omega, \tau')}} = i\omega \int_0^\tau \left[ \frac{1}{\sqrt{A}} - \frac{iB}{2A\sqrt{A}} \right] d\tau' = \int_0^\tau \left[ \frac{i\omega}{\sqrt{A}} + \frac{\omega B}{2A\sqrt{A}} \right] d\tau' \quad (15)$$

Assume now the following boundary condition:  $K=0$  when  $\tau \geq T$ . Integration of Eq. (25) now gives the solution

$$-K(\omega, \tau) \exp(-\phi(\omega, \tau)) = -\int_\tau^T r(\tau') \exp(-\phi(\omega, \tau')) (1 - K^2(\omega, \tau')) d\tau' \quad (16)$$

From Eq.(27) we can, when  $K^2 \ll 0$ , obtain the non-linear solution

$$K(\omega, \tau) = \exp(\phi(\omega, \tau)) \int_{\tau}^T r(\tau') \exp(-\phi(\omega, \tau')) (1 - K^2(\omega, \tau')) d\tau' \quad (17)$$

Equation (28) is now the starting point for a non-linear modelling algorithm. Assume a discretization in  $\tau$  (sample interval  $\Delta\tau$  and total of  $N$  points), and then start at maximum time  $T=(N-1) \Delta\tau$  and then calculate  $K$  in upward direction.

We introduce the following notation for convenience

$$\begin{aligned} K_{i,j}^n &= K^n(\omega_i, \tau_j) \quad \tau_j = (j-1)\Delta\tau, \quad j = N-1, N-2, \dots, 1 \\ K_{i,N}^n &= 0 \end{aligned} \quad (18)$$

Where the superscript  $n$  implies iteration number.

Next, define (trapezoidal rule applied to integral in Eq.(28)) (assume  $(n+1)$  th. iteration)

$$\begin{aligned} \beta_{i,j} &= \frac{\Delta\tau}{2} \left[ r_{j+1} X_{i,j+1} \{1 - (K_{i,j+1}^n)^2\} + r_j X_{i,j} \{1 - (K_{i,j}^n)^2\} \right], \quad j = N-1, N-2, \dots, 1 \\ r_N &= 0 \end{aligned} \quad (19)$$

Which gives the after sought solution

$$K_{i,j}^{n+1} = \beta_{i,j} / X_{i,j}, \quad j = N-1, N-2, \dots, 1 \quad (20)$$

In Eqs.(18 and 19) we have introduced the operator

$$X_{i,j} = \exp[-\phi(\omega_i, \tau_j)] \quad \tau_j = (j-1)\Delta\tau \quad (21)$$

The seismogram corresponds to the solution  $j=1$ . The final result in time is obtained after an inverse FT.

Let the first layer be water, then we need to include the free-surface multiples. Assume that  $\tau_\omega$  represents two-way vertical travel time in the water layer. Total field  $P_i$  recorded at the surface (e.g. including multiples) can then be written as ( $r$  being the reflection coefficient of the seafloor)

$$P_i = K_{i,j=1} \left[ 1 - r \exp(-i\omega_i \tau_\omega) + r^2 \exp(-2i\omega_i \tau_\omega) + \dots = \frac{K_{i,j=1}}{1 + r \exp(-i\omega_i \tau_\omega)} \right] \quad (22)$$

## Forward numerical implementation

When we make calculations with the models we need to define  $r(\tau)$  from a set of layered model parameters connected to the impedance of a seismic media. We can, of course, get  $r_j$  from eq (22) as reflectivity per depth unit (1/s). Invoking Eq.(23) we can calculate two-way traveltimes by converting the layer thickness  $z$  into time and using:

$$r(\tau) = \frac{1}{2(\tau_{j+1} - \tau_j)} \left[ \frac{\rho_{j+1} v_{j+1}}{\rho_j v_j} - 1 \right] \quad j=1, \dots, NT-1 \quad (23)$$

We can then get  $R_j$  (Reflection coefficients) either by setting  $\rho$  and  $v$  direct into Eq.(24) or setting  $r$  from Eq (23) into Eq.(24). Both  $r$  and  $R$  are similar physical parameters which represents the contrast in acoustic impedance across an interface. To proceed with computations we must discretize every layer in the model with  $j$  and move down to the layer  $NT-1$ . Velocity and density for each layer we find in table 2.a:

$$R_j = \frac{\rho_{j+1} v_{j+1} - \rho_j v_j}{\rho_{j+1} v_{j+1} + \rho_j v_j} = \frac{\exp[2\Delta\tau r_{j+1}] - 1}{\exp[2\Delta\tau r_{j+1}] + 1} \quad \text{for } j = 0, 1, 2, \dots, NT - 1 \quad (24)$$

| $Q$ | $Z$ (Depth) | Density $\rho$ g/cm <sup>3</sup> | Velocity $v$ km/h |
|-----|-------------|----------------------------------|-------------------|
| 200 | 600         | 1.9                              | 4500              |
| 50  | 200         | 2.2                              | 5000              |
| 200 | 400         | 2.4                              | 3200              |
| 50  | 200         | 2.3                              | 5000              |
| 200 | 500         | 2.3                              | 4500              |

Depth z (m)

|         |
|---------|
| Layer 1 |
| Layer 2 |
| Layer 3 |
| Layer 4 |
| Layer 5 |

Table 2.a. Seismic model parameters

The solution of eq.(17) gives the iteration procedure in a downward continuation process similar to Nilsen and Gjevik in the forward case. However, we now have a general Q-model and not only the Kelvin Voigt model. The crucial point in this procedure is that the term proportional to  $K$  squared on the right hand side of eq. (17) is regarded to be small. In the first approximation this term is therefore neglected and in each of the higher order approximations the previous determined approximation to  $K$  is substituted for  $K$  in the right hand side of eq.(17).

I used the data from table 2.a in my two previous articles Sørdsdal (2018) and Sørdsdal (2) (2018). In the last article I introduced free surface multiples in the iterative solution. The multiples were easily introduced. However, to be correct, to introduce free surface multiples requires a water layer above the other layers as introduced in Eq.(22). Density of the water layer is 1 g/cm<sup>3</sup> and velocity is 1480 km/h. So, to introduce free surface multiples in the correct way I will also come up with a second model (table 2.b) that starts with a correct water layer. It would not be a good idea simply to add a water layer to Table 2.a. We have to adopt the layers under the water layer so we will get a solution that converges.

| $Q$ | $Z$ (Depth) | Density $\rho$ g/cm <sup>3</sup> | Velocity $v$ km/h |
|-----|-------------|----------------------------------|-------------------|
| 200 | 600         | 1.0                              | 1480              |
| 200 | 200         | 1.5                              | 2000              |
| 200 | 400         | 2.0                              | 2180              |
| 200 | 200         | 1.9                              | 1950              |
| 200 | 500         | 2.0                              | 2200              |

Table 2.b. Seismic model parameters

Fig.3 shows solutions for eq.(17) (left) in the undamped (black) and damped (red) case. We have used the absorption model of Wang (model 1 in Table 1  $\omega_h=140$  Hz) and the parameters from Table 2.b. Here we can see the reflectors after transmission loss and with interbed multiples as well as free surface multiples. To the right we have eq.(22) that also includes free surface multiples.

For the removal of free surface multiples we have, as mentioned, Eq.(22). If we assume that  $t_w$  represents two-way vertical travel time in the water layer, the total field  $P_1 = P(w_1)$  recorded at the receiver including multiples can then be written as Eq.(22), and we will introduce water bottom multiples in K simply by multiplying K with P in the forward computations. To remove multiples in the inversion we simply multiply the inverted K with the inverse of P.

From fig.3 we have a good reconstruction of what we expected and we can conclude that the solution Eq. (17) gives us a good solution of the Riccati-equation in the forward case.

We have shotpulse  $f_c = 60$ Hz. (Appendix A13). The solution without absorption was also done by Gjevik. However, we have added free surface by solving Eq. (22) that Gjevik did not do. And we also added absorption.

Left plot is the solution with multiples, transmission loss and absorption, simply the solution of Eq.(17). Right plot is with free surface multiples included.

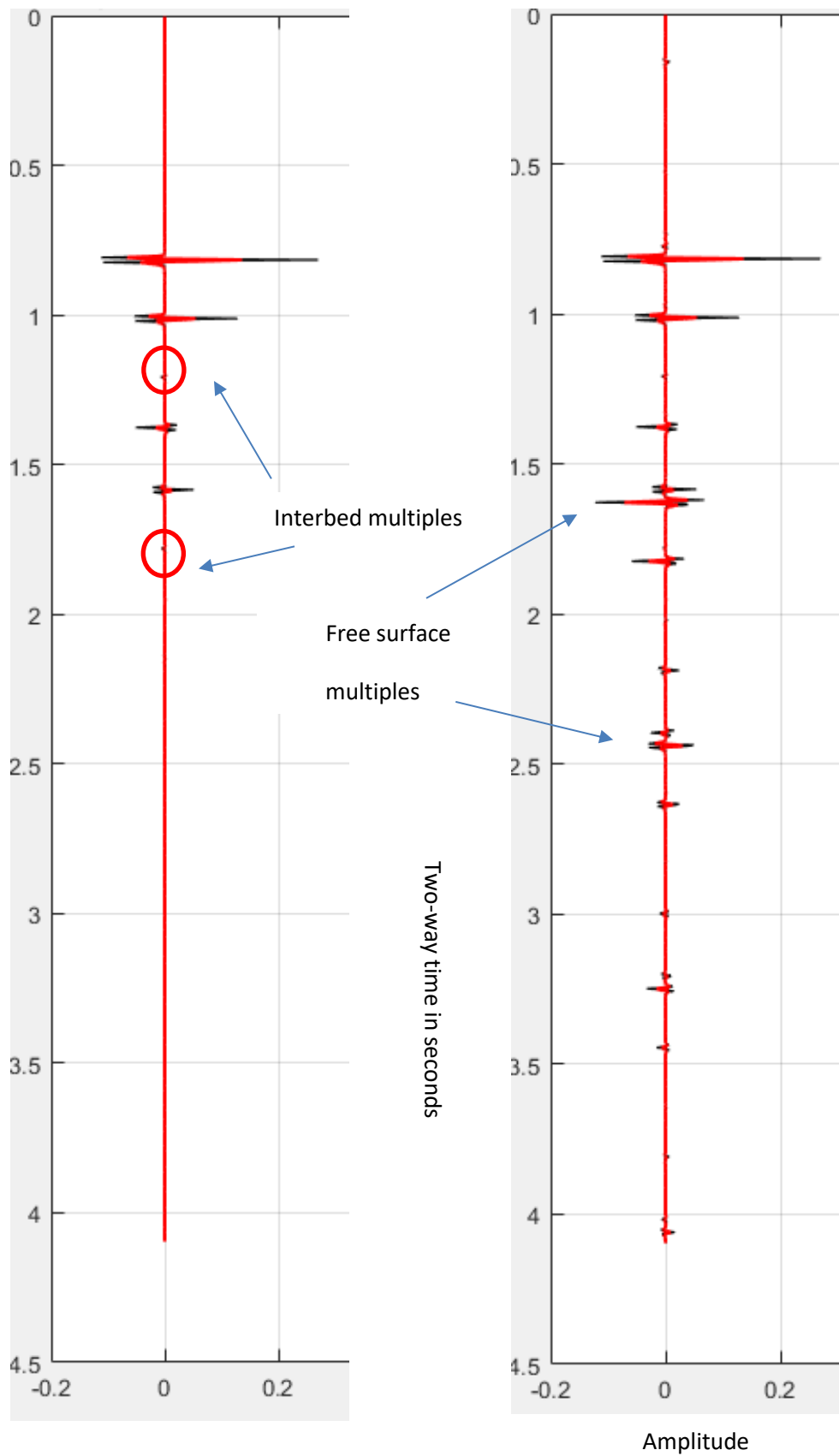


Fig.3 .From left, Reflectors with shotpulse 60 Hz. Q-filtered (red) no Q-filter (black) middle Eq. (17) with interbed multiples. Right Eq.(22 with interbed multiples and free surface multiples

Before we jump to the inversion, we need to give a remark about the impedance. The relation between  $r$  and the impedance makes it possible to compute the impedance for every solution of  $r$ . If the acoustic impedance  $I_0$  is known at  $z = 0$ , (or at any depth),  $I$  is also uniquely determined as a function of  $\tau$ . From Eq. (11) we can deduce:

$$I = I_0 \exp\left(2 \int_0^{\tau} r(\tau') d\tau'\right) \quad (25.b)$$

where  $I_0 = \rho_0 v_0$  and  $I = \rho v$ .  $I/I_0$  will give us a dimensionless relative impedance. We will come back to this in the next section.

## Inverse-Q filtering – inverse numerical implementation

In the following we will implement the layered model parameters (Table 2.b) that was used to generate the synthetic seismograms in the forward modeling above. The inversion will be done taking the forward modelled synthetic seismograms as input. The procedure will be done both with a conventional least square seismic inversion procedure and with downward continuation using inverse Q-filtering models. In the first procedure we will use only forward Q-filtering models and not use inverse Q-filtering at all. The second approach use the inverse of the models in Table 1.

Consider Eq. (17) in the limit  $\tau \rightarrow 0$ , which gives the ‘seismogram’

$$K(\omega, 0) = \int_0^T r(\tau') \exp(-\phi(\omega, \tau')) (1 - K^2(\omega, \tau')) d\tau' \quad (26)$$

Introduce ‘reflectivity’ series

$$r(\tau) = \Delta\tau \sum_{i=0}^{NT-1} r_i \delta(\tau - i\Delta\tau), T = NT \cdot \Delta\tau \quad (27)$$

Combination of Eqs. (26) and (27) gives

$$K(\omega, 0) = \sum_{i=0}^{NT-1} r_i \exp(-\phi(\omega, i\Delta\tau)) (1 - K^2(\omega, i\Delta\tau)) \Delta\tau \quad (28)$$

Originally, seismogram recorded in timedomain, i.e.  $k(t, 0)$ , and assume sampled with a total of  $NT$ -samples. Fourier transform of the data will give the same number of monochromatic seismograms.

Nilsen and Gjevik introduced an iterative inversion procedure to solve for  $r$  in eq.(26) when the reflection response of the reflecting layer is known. When absorption was included that could be a complicated process and as far as we know no calculations were done with absorption by them.

Gelius, in an unpublished note, suggested a more elegant solution of the equation with the matrix system:

$$\begin{bmatrix} K_{n+1}(\omega_0, 0) \\ K_{n+1}(\omega_1, 0) \\ \cdot \\ \cdot \\ K_{n+1}(\omega_{NT-1}, 0) \end{bmatrix} = \tag{29}$$

$$\begin{pmatrix} \exp(-\varphi(\omega_0, 0)(1 - K_{0,n}^2) & \exp(-\varphi(\omega_0, \Delta\tau)(1 - K_{1,n}^2) & \dots & \exp(-\varphi(\omega_0, (NT-1)\Delta\tau)(1 - K_{n,n}^2) \\ \exp(-\varphi(\omega_1, 0)(1 - K_{0,n}^2) & \exp(-\varphi(\omega_1, \Delta\tau)(1 - K_{1,n}^2) & \dots & \exp(-\varphi(\omega_1, (NT-1)\Delta\tau)(1 - K_{n,n}^2) \\ \cdot & \cdot & \dots & \cdot \\ \cdot & \cdot & \dots & \cdot \\ \cdot & \cdot & \dots & \cdot \\ \exp(-\varphi(\omega_{NT-1}, 0)(1 - K_{0,n}^2) & \exp(-\varphi(\omega_{NT-1}, \Delta\tau)(1 - K_{1,n}^2) & \dots & \exp(-\varphi(\omega_{NT-1}, (NT-1)\Delta\tau)(1 - K_{n,n}^2) \end{pmatrix} \begin{pmatrix} r_{n,0} \\ r_{n,1} \\ \cdot \\ \cdot \\ r_{n,NT-1} \end{pmatrix}$$

Hagos (2016) made some computations for Eq.(29) in his thesis. A more detailed study of the solution is in appendix 2. The mathematics for how to do least square inversion is also outlined in Sørdsal (2) (2018).

Note that  $K_0^2=0$  in the first iteration. After a new estimate of the reflectivity series has been obtained, an update of  $K_{i,n}^2$  can be obtained by solving the forward problem. Iterations are carried out until the relative change in reflectivity is below a certain user threshold. The effect of the inversion when  $K^2 = 0$  is simply to compensate for the damping of the amplitude caused by attenuation and correct the phase term caused by dispersion. When  $K^2 \neq 0$  we also remove multiples and compensate transmission loss. Surface multiples can also be removed simply by multiplying  $K$  with the inverse of RHS of Eq (22). First we remove surface multiples before we solve Eq.(29). This can simply be done multiplying  $r$  with the inverse of Eq. (22)

The solution to Eq.(29) after inversion will be important for further study. The idea of the inversion is to compare the impedance from the seismic model (table 2.a and b) with the impedance after the inversion. The success of the inversion depends on how close the impedance we compute from the inverted data are to the impedance from the model data.

Fig.4. a. and b shows a solution  $r$  after 1.iteration and after 5 iterations, and with parameters from table 2.a. and b. Surface multiples are removed simply by multiplying  $r$  with the inverse of Eq. (22). Then in further iterations interbed multiples are removed so both interbeds and surface multiples are removed in the final solution. (middle graph red).

The impedance-inversion, graph 4 from left, gives a good picture of the inversion. Blue dotted graph gives relative impedance for 1. iteration. Red graph indistinguishable from black dotted graph shows 5. Iteration plotted on the model. The reflectors for the model are on the most right plot.

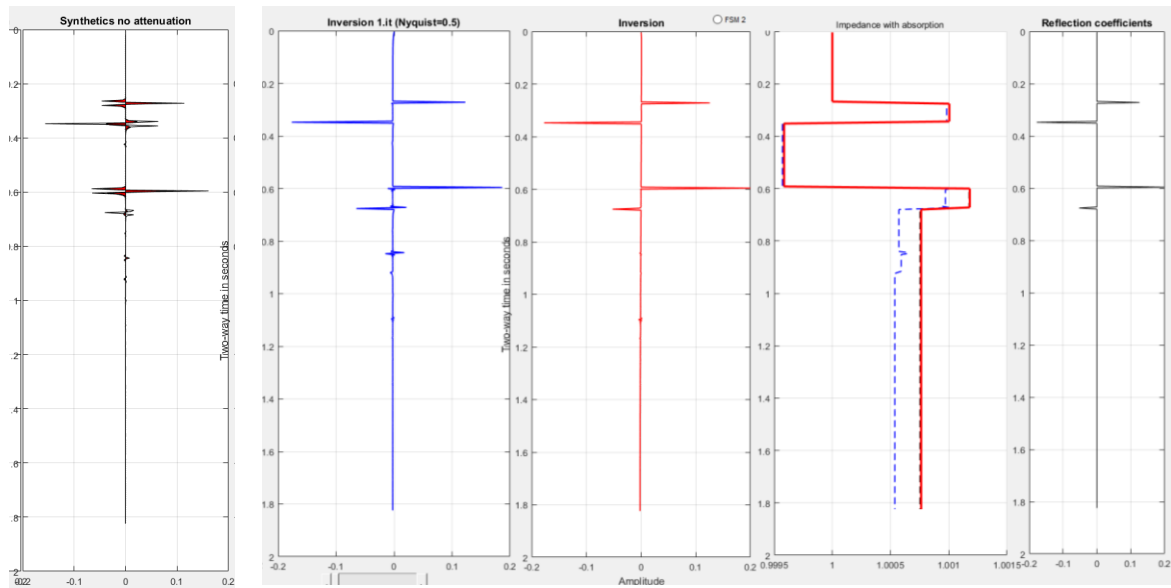


Fig.4.a. Data from table 2.a. From left: Synthetics with interbed multiples (Absorption model 1). Then inversion 1.it (blue), then full inversion (red) and then impedance inversion with corresponding colors. Full inversion is indistinguishable from the model. (black dotted). Right plot: reflection coefficients for the model.

Fig.4.a. shows that model parameters 2.a gave us a good inversion removing, interbed multiples and restoring transmission loss. The shot pulse and absorption were also removed in the final solution. Fig.4.b. shows that with parameters from table 2.b, the interbed multiples are small and barely visible on the figure, free surface multiples however are generated and removed in the inversion.

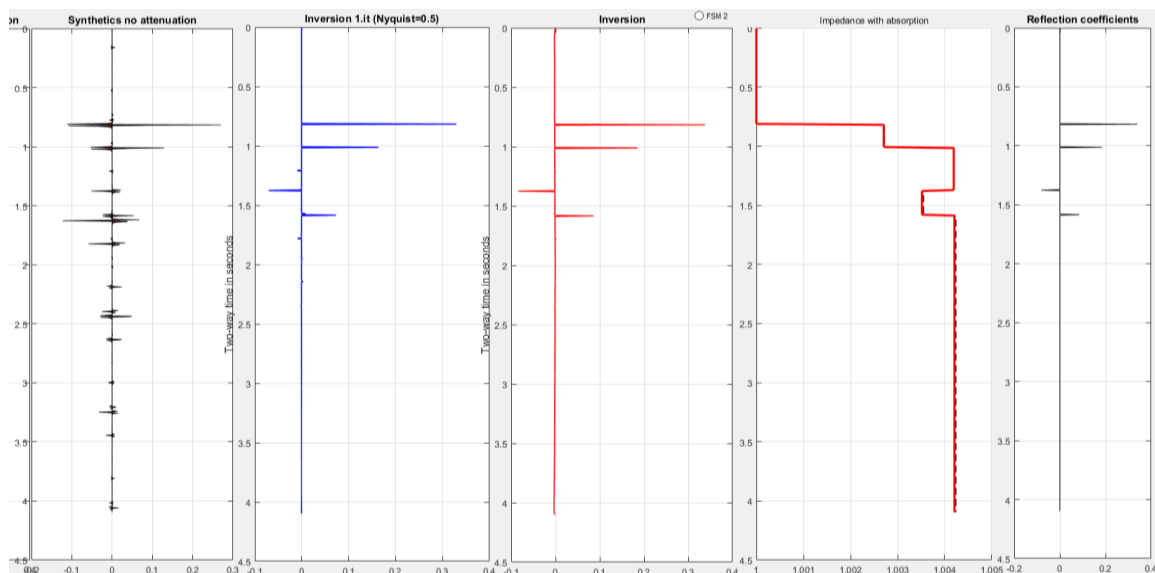


Fig.4.b.data from table 2.b. From left: Synthetics with free surface multiples (Absorption model 1). Then inversion 1.it (blue), then full inversion (red) and then impedance inversion where colors corresponds with previous plots . Full inversion is indistinguishable from the model. (black dotted). Right plot: reflection coefficients for the model.

## Inverse Q-filtering with downward continuation

Solving the inverse problem in the last section is time-consuming because it involves the computation of an inverse matrix. The theory of Nilsen and Gjevik was a theory of inversion without an inverse matrix in the sense of LSQ. This was because inversion theory was not developed as far as today's LSQ-matrix theory in MATLAB at the time their article was published. However, a hint was given that a solution can be given by deconvolution. To achieve deconvolution we apply inverse Q-filtering (IQF). Computation with IQF is not done in this paper, but I plan to do it later.

Now, let us discuss Gjevik's theory by a simpler approach than the LSQ-matrix Eq (29). We drop the free surface multiples (as Gjevik also did), and start with the forward solution Eq (17). In addition to Nielsen and Gjevik's approach our phase function represents a general viscoelastic absorption model and not only the Kelvin Voigt model. The inversion procedure closely follows Nilsen and Gjevik's paper.

If the reflection response  $K$  and the viscoelastic properties of the medium are known,  $r$  can be computed by an inversion iteration procedure. We simply multiply Eq (17) by  $\frac{1}{2\pi} \exp(i\omega t)$  and integrate with respect to  $\omega$ . By interchanging the sequence of integration, we obtain:

$$\int_0^T r(s)H(t-s, s)ds = \frac{1}{2\pi} \int_{-\infty}^{\infty} K(0, i\omega) \exp(i\omega t) d\omega + \frac{1}{2\pi} \int_0^T r(s) \int_{-\infty}^{\infty} K^2 \exp(i\omega t) \exp(-\Phi(s, i\omega)) d\omega ds \quad (30)$$

The function  $H$  in equation (30) represents attenuation and is equivalent to the function  $H$  in Nilsen and Gjevik's paper. Our function, however, is a general viscoelastic filterfunction that must be defined for each Q-model separately.

In the case of no energy absorption, the function  $H$  approaches the delta function and the left hand side of equation (30) is simply  $r(t)$ . We now have a straight forward method to find the reflection response including absorption for a great variety of viscoelastic models when  $r(t)$  and the viscoelastic model is given.

Our first attempt of inversion will be for the 1.iteration, neglecting the second term on RHS of Eq (30). If we develop our theory for the 1.iteration also in the modeling, we will neglect the term  $K^2$  in eq(17). Then we will have a theory simply for forward and inverse Q-filtering of a linear kind. Eq (30) with  $K^2 = 0$  is then similar to the downward continuation method discussed by Wang (2007). Wang has implemented the Kolsky-model both as a forward Q-filter and an inverse Q-filter that he calls modified Kolsky. Table 3 shows the different inverse Q-models that corresponds to the forward Q-models of table 1. Model 1 (Wang-Kolsky) is presented on page 94 in Wang's book. (Wang (2008)).

Wang simply changed the sign for the exponential in the forward Q-model to achieve the inverse. Futterman causal is wellknown. Futterman non causal and Kelvin Voigt can be achieved simply by changing the sign of the Q-value.

| Model                  | A   | B   |
|------------------------|---|---|
| 1 Wang Kolsky          | $\left[\frac{\omega}{\omega_h}\right]^{-2\gamma}$ | $\left[\frac{\omega}{\omega_h}\right]^{-2\gamma} \frac{1}{Q}$ |
| 2 Futterman non-causal | 1   | $-\frac{1}{Q}$  |
| 3 Kelvin Voigt         | 1   | $-\omega \frac{q}{\rho v_r^2}$                                |

Table 3 Inverse Q-filter models

## Solution with LSQ, FQF and IQF

Up till now we have achieved three important goals:

1. We have applied a general Q-filter to the Riccati-equation and not only the Kelvin-Voigt model. Sørsdal (1981)
2. We have connected the Riccati-equation with Q-filtering to Wang's downward continuation method with Q-filtering described in his book. Wang (2008).
3. Finally, by reaching the two goals above, we also have introduced non-linearity to the theory of downward continuation with Q-filtering by Wang.

Now we have an elegant method to study forward and inverse Q-filtering by using LSQ, FQF and IQF for many different variables in the models.

To start with LSQ, the solutions on fig.4 a and b are a complete solution and very accurate inversion for our seismic model. We can call this the LSQ-inversion. Fig.5 shows the LSQ-inversion after 5. iterations for absorption model 1 (Wang Kolsky) and model parameters from table 2.a. This is the same inversion as depicted in fig.4.b. Left plot (red) gives r with Eq. (29) as complete and accurate LSQ-solution. Then green plot gives solution r with Gjevik's solution Eq. (30) after 5 iterations and absorption model 1 ( $\omega_h = 140\text{Hz}$ ). If we do not use LSQ we must consider the shotpulse removed. However, as long as the inverse filter LHS in the equation is not implemented we did not get r fully restored as we did with LSQ. The impedance inversion to the right corresponds to the colors in the left plot.

So, in this case we must use FQF and IQF to modify the final solution. We should expect a better solution with IQF as I plan to do in a later paper. And we also could expect an alternative solution with another choice of FQF.

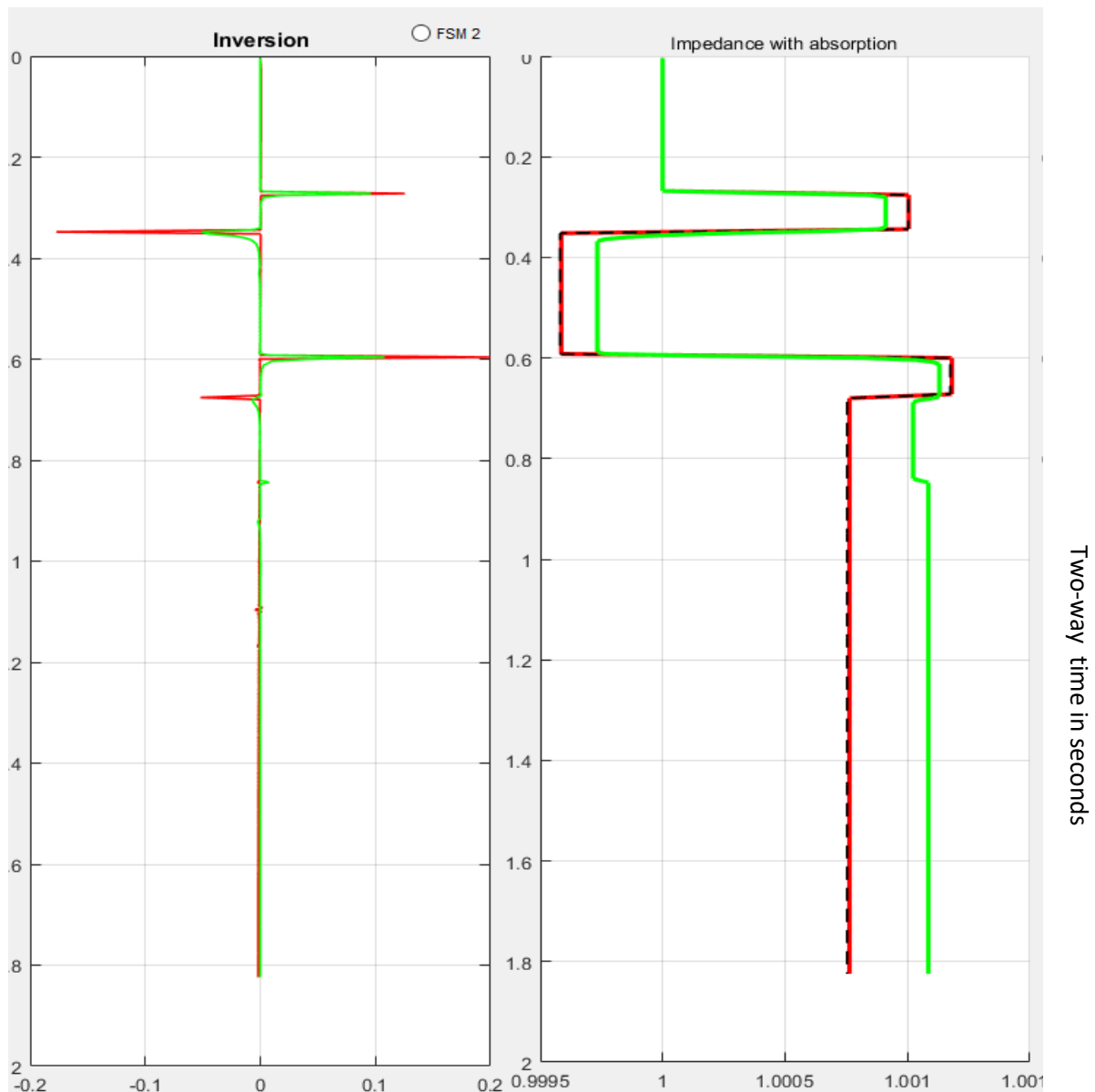


Fig.5 Left: .LSQ-inversion for absorption model 1 (red) and the inversion of Gjevik without IQF and LSQ (green). Impedance-inversion right graph where colors corresponds with left graph.

So, let us first try another FQF (table 1). Actually, we could discuss the effect of the FQF when we do not use LSQ, and get a good view of all different filters. (LSQ, FQF and IQF). The second term of RHS of Eq.(30) will represent the FQF filtered part of Gjevik's solution. The inversion and the impedance inversion are on fig.6. We can see that even though the impedance inversion for different FQF-models are very close to the model, we did not get as good solution as with the LSQ on fig.4.b. Green plot is solution with absorption model 1, and the other plots are with model 2 (Futterman non-causal).

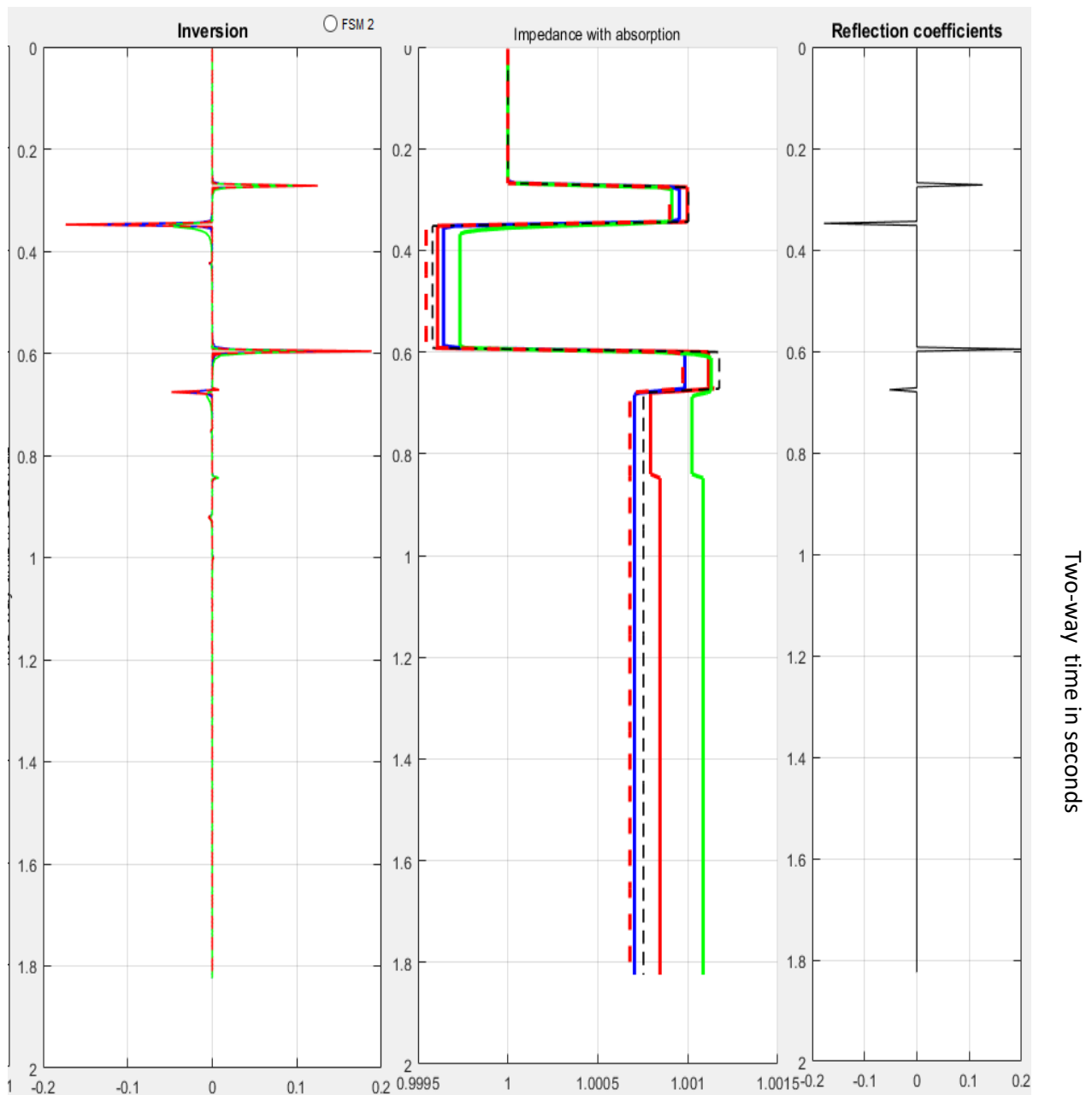


Fig.6. Left: Inversion for Gjevik's solution. Right: Impedance inversion. Colors corresponding Red: Model 2 zero damping. Green: model 1,  $\omega_h=140$  Hz. Blue: Model 2  $Q=250$  Red stipled: Model 2  $Q=500$ . Black stipled is the model (reflections right)

## Inversion with IQF

To sum up, we got a very good solution with LSQ, indistinguishable from the model. Then implementing FQF without LSQ we got solutions that could be improved by the right choice of absorption parameters and absorption model. And the solutions that worked well with the right FQF, should be improved further by IQF. I will not do calculations with IQF in this article, but do it in a later article. We have seen that in cases where we will not use LSQ we will get a fairly good inversion using the right FQF and in this case probably save some computation time.

To further sum up, the impedance-inversion and the regular inversion for the LSQ-solution and the Gjevik/Nielsen's solution is shown on Fig.5-6. The solution has some similarity with the LSQ-solution. Since Wang's Kolsky model was used in the solution a better solution could be done by applying the inverse absorption models from table 3.

Ultimately, after the development of the previous theory we have been able to set up all different forward and their associated inverse Q filters. To link the downward continuation theory presented in Wang to the matrix representation Eq (29) we state that the theory as wavefield downward continuation, can represent downward continuation as a linear system uniformly in a vector-matrix form.

Therefore setting  $K^2=0$  in eq (29) we achieve the linear solution on matrix form and can solve this for  $r$  as a time-domain vector that represents the filter. The inverse Q-filtering procedure must be performed successively to each time sample to get the time-dominant output vector. We then use the output  $r$  as input getting the inverted solution for a new inverted  $r$ . When we do this we replace the Q-filters applied in the phase function  $\phi$  with the inverse Q-filters from table 3. Further iterations introduce non-linearity on the way to a seismic theory that can be used on real data.

## Conclusion

The results of the preceding sections show that the Riccati equation with Q-filtering provides a method for the construction of synthetic reflection seismograms that is a continuation of the method introduced by Nilsen and Gjevik. Moreover does this theory describe a method for inverting reflection data, i.e. computing the variations in the acoustic impedance within a reflecting layer that can be used in real prospecting. This I have briefly suggested by introducing a water layer in the seismic model. And the Riccati inversion corrects phase, compensates frequency loss, removes multiples and compensates transmission loss in one single process.

So far we have tested the abilities of the inversion method by inverting a synthetic reflection seismograms computed from a simple impedance model underneath a water layer. It would, however – as Gjevik suggested several years ago - be interesting to apply the present inversion method to real reflection data from a more complex structure. A number of problems will then arise as was discussed in the paper of Nilsen and Gjevik. However, because of years of rapid development in inversion theory, this is much easier solved today than when the theory first was introduced .

Even if this could be done only with a limited degree of accuracy, the main problem is, however, that what Gjevik asked is not fully answered: will one lose so much information or introduce so many errors through this process that the inversion becomes meaningless when applied to real prospecting? In view of the success of the introduction of inverse Q-filtering this could soon be answered and we plan to study these problems in the future.

## Acknowledgement

It is a pleasure for me to express my gratitude to professor emeritus Bjørn Gjevik at the University of Oslo who first introduced me to the inversion with the Riccati equation. I will thank him for help and advice all the way through the application of this modification of his original theory. I will also thank professor Leiv Gelius at the university of Oslo who wrote a part of the basic MATLAB-program and gave valuable hints on how to use the program in my own research.

**References**

- Gjevik et al. (1976) *An attempt at the inversion of reflection data. Geophysical prospecting* 24,492-505
- Nielsen and Gjevik (1978): *Inversion of reflection data. Geophysical prospecting* 26, 421-432
- Yanghua Wang (2008) *Blackwell Publishing. Seismic inverse Q filtering*
- Knut Sørdsdal (1981) *Viskoelastiske dempningsmodeller i Riccatiligningen anvendt i marin seismikk. University of Oslo*
- Knut Sørdsdal (2018) *1-D non-linear inversion of data with absorption - revisited.*  
[https://www.researchgate.net/publication/331257025\\_1-D\\_non-linear\\_inversion\\_of\\_data\\_with\\_absorption\\_-\\_revisited](https://www.researchgate.net/publication/331257025_1-D_non-linear_inversion_of_data_with_absorption_-_revisited)
- Knut Sørdsdal (2) (2018) *Reflections on non-linear seismic inversion*  
[https://www.researchgate.net/publication/332233629\\_Reflections\\_on\\_non-linear\\_seismic\\_inversion](https://www.researchgate.net/publication/332233629_Reflections_on_non-linear_seismic_inversion)
- Bland(1960) *The theory of linear viscoelasticity. Pergamon Press*
- Horton (1959) *A loss mechanism for the Pierre Shale. Geophysics vol.24, no 4*
- Aki and Richards (2002) *Quantitative Seismology W.H. Freeman and Co. San Fransisco*
- Kolsky, 1956 *The propagation of stress pulses in viscoelastic solids. Philosophical Magazine* 1, 693-710
- Kjartansson E. 1979 *Constant Q wave propagation and attenuation. Journal of Geophysical Research* 84 4737-48.
- Futterman W.I 1962 *Dispersive body waves. Journal of Geophysical Research* 67 , 5279-91
- Trorey A.W, 1962 *Theoretical seismograms with frequency and depth dependent absorption. Geophysics* 27, 766-85
- Claerbout J.F.1976 *Fundamentals of Geophysical Data Processing. McGraw-Hill Book Co. New York*
- Hagos Geberehiwet Gebregergs (2016):*Compensation of Absorption Effects in Seismic Data. University of Oslo*

### Appendix 1

In the literature the wavenumber  $k$  is often written on the following form in case of absorption (constant-Q model)

$$k = \frac{\omega}{v(\omega)} \left[ 1 - \frac{i}{2Q} \right] = \frac{\omega}{v_r} + \left[ \frac{\omega}{v(\omega)} - \frac{\omega}{v_r} \right] - i\alpha(\omega) = \frac{\omega}{v_r} + \varphi(\omega) - i\alpha(\omega). \quad \alpha = \frac{\omega}{2Qv(\omega)} \quad (\text{A.1})$$

Where  $\alpha$  is the absorption coefficient and  $\varphi$  is the phase of the ‘absorption filter’. In order to ensure causality, the filter should be minimum phase. For such a filter this relationship holds.

$$\varphi(\omega) = \text{H}[\alpha(\omega)]$$

With H denoting the Hilbert Transform. In case of no dispersion ( $\varphi=0$ ), the filter will be noncausal. Then we have

$$k = \frac{\omega}{v_r \sqrt{Y}} = \frac{\omega}{v_r \sqrt{A + iB}} = \frac{\omega}{v_r} \left[ \frac{1}{\sqrt{A}} - \frac{i}{2} \frac{B}{A\sqrt{A}} \right] \quad (\text{A.2})$$

Equating Eqs. (A.1) and (A.2) gives the relationships

$$A = \left[ \frac{v(\omega)}{v_r} \right]^2 \quad B = \left[ \frac{v(\omega)}{v_r} \right]^2 \frac{1}{Q}, \quad (\text{A.3})$$

Aki and Richards (2002) show that the following relation should be held to honor causality

$$\frac{\omega}{v(\omega)} - \frac{\omega}{v_\infty} = \text{H} \left[ \frac{\omega}{2Qv_\infty} \right] \quad (\text{A.4})$$

Where  $v_\infty$  is the limit of the velocity function when  $\omega$  tends to infinity. Equation (12) can be further approximated as

$$\frac{\omega}{v(\omega)} - \frac{\omega}{v_h} \cong \text{H} \left[ \frac{\omega}{2Qv_\infty} \right] \quad (\text{A.5})$$

Where  $v_h$  is the velocity related to the highest possible (tuning) frequency of the seismic band. The wavenumber is accordingly adjusted as (compare with Eq.(A.1)).

$$k = \frac{\omega}{v_h} + \left[ \frac{\omega}{v(\omega)} - \frac{\omega}{v_h} \right] - i \frac{\omega}{2Qv(\omega)} = \frac{\omega}{v_h} \left\{ 1 + \left[ \frac{v_h}{v(\omega)} - 1 \right] - i \frac{v_h}{2Qv(\omega)} \right\} \quad (\text{A.6})$$

And combined with a Kolsky type of phase-velocity model (Kolsky, 1956)

$$v(\omega) = v_h \left( \frac{\omega}{\omega_h} \right)^\gamma, \quad \gamma = (\pi Q)^{-1} \quad (\text{A.7})$$

Gives the wavenumber model

$$k = \frac{\omega}{v_h} \left[ 1 + \left[ \left( \frac{\omega}{\omega_h} \right)^{-\gamma} - 1 \right] - \frac{i}{2Q} \left( \frac{\omega}{\omega_h} \right)^{-\gamma} \right] \quad (\text{A.8})$$

Which has been employed by Wang. From Eqs. (A.1) and (A.2) it also follows that ( $v_r=v_h$ )

$$A_{Wang} = \left[ \frac{\omega}{\omega_h} \right]^{2\gamma} B_{Wang} = \left[ \frac{\omega}{\omega_h} \right]^{2\gamma} \frac{1}{Q} \quad (\text{A.9})$$

From Eq.(A.9) it follows that  $0 < A_{Wang} < 1$ , and the same for  $B_{Wang}$  but with  $B_{Wang} \ll A_{Wang}$ .

Based on Eq. (A.3), Kjartansson (1979) proposed an alternative wavenumber model

$$k = \frac{\omega}{v_\infty} + \left[ \frac{\omega}{v(\omega)} - \frac{\omega}{v_\infty} \right] - i \frac{\omega}{2Qv_\infty} = \frac{\omega}{v_\infty} + H \left[ \frac{\omega}{2Qv_\infty} \right] - i \frac{\omega}{2Qv_\infty} \quad (\text{A10})$$

From Eqs.(11) and (A.10) it follows that ( $v_r=v_\infty$ )

$$A_{Futt} = \left[ 1 + \frac{1}{\omega} H \left( \frac{\omega}{2Q} \right) \right]^{-2} B_{Futt} = (A_{Futt})^{3/2} \frac{1}{Q} \quad (\text{A.11})$$

For completeness, we also have the dispersion-free and non-causal absorption model of Futterman (1962), which corresponds to

$$A_{Futt} = 1 \quad B_{Futt} = \frac{1}{Q}$$

### Ricker wavelet in the synthetics

In order to get the synthetic seismogram in time domain by inverse Fourier transform of the complex reflection coefficient K, each component of K (Eq.(26) is multiplied by a sampled Ricker wavelet in frequency domain:

$$Srw = (2/(\sqrt{\pi})) \frac{f^2}{f_c^3} \exp\left(-\frac{f}{f_c}\right)^2 \quad (\text{A.13})$$

This Ricker wavelet is a zero-phase wavelet and is non-causal. The frequency  $f_c$  is called the center frequency and will vary.

**Appendix 2**

To apply least-square inversion, Eq. (29) can be written in vector and matrix notation in short as

$$\vec{K} = M \vec{r} \quad (\text{A14})$$

where

$$\vec{K} = \begin{bmatrix} K_{n+1}(\omega_0, 0) \\ K_{n+1}(\omega_1, 0) \\ \vdots \\ K_{n+1}(\omega_{NT-1}, 0) \end{bmatrix} \quad \vec{r} = \begin{bmatrix} r_{n,0} \\ r_{n,1} \\ \vdots \\ r_{n,NT-1} \end{bmatrix}$$

$$M = \Delta\tau \begin{pmatrix} \exp(-\varphi(\omega_0, 0)(1 - K_{0,n}^2)) & \exp(-\varphi(\omega_0, \Delta\tau)(1 - K_{1,n}^2)) & \dots & \exp(-\varphi(\omega_0, (NT-1)\Delta\tau)(1 - K_{n,n}^2)) \\ \exp(-\varphi(\omega_1, 0)(1 - K_{0,n}^2)) & \exp(-\varphi(\omega_1, \Delta\tau)(1 - K_{1,n}^2)) & \dots & \exp(-\varphi(\omega_1, (NT-1)\Delta\tau)(1 - K_{n,n}^2)) \\ \vdots & \vdots & \dots & \vdots \\ \vdots & \vdots & \dots & \vdots \\ \exp(-\varphi(\omega_{NT-1}, 0)(1 - K_{0,n}^2)) & \exp(-\varphi(\omega_{NT-1}, \Delta\tau)(1 - K_{1,n}^2)) & \dots & \exp(-\varphi(\omega_{NT-1}, (NT-1)\Delta\tau)(1 - K_{n,n}^2)) \end{pmatrix} \quad (\text{A15})$$

$\vec{K}$  is a (Nx1) vector, M is a (NxN) matrix and  $\vec{r}$  is a (Nx1) vector. Let  $\vec{K}$  be the desired seismic output data while the actual output from Eq. (A14) is  $\vec{S} = M \vec{r}$ . We want to compute a reflectivity per depth unit series  $\vec{r}$  such that the difference  $\vec{\Sigma}$  between the actual output  $\vec{S}$  and the predicted seismic output data  $\vec{K}$  is minimum in the least square sense. Therefore, the error  $\vec{\Sigma}$  with respect to parameter vector  $\vec{r}$  is  $\vec{\Sigma} = \vec{K} - \vec{S} = \vec{K} - M\vec{r}$ . And the cumulative squared error:

$$\vec{\Sigma}^T \vec{\Sigma} = (\vec{K} - M\vec{r})^T * (\vec{K} - M\vec{r}) =$$

$$(\vec{K}^T * \vec{K} - \vec{K}^T M\vec{r}) - r^T M^T K^T + (\vec{r}^T M^T * M\vec{r}) \quad (\text{A16})$$

Where T denotes matrix transpose and \* denotes complex conjugate.

We want to estimate a reflectivity per depth unit series  $\vec{r}$  such that the quantity  $\vec{\Sigma}^T \vec{\Sigma}$  is minimum. This condition leads to setting the derivative of  $\vec{\Sigma}^T \vec{\Sigma}$  with respect to  $\vec{r}$  to zero. Differentiate both sides of eq. (A16) with respect to  $\vec{r}$  and observe the requirement for least square procedure minimization that

$$\frac{\delta \vec{\Sigma}^T \vec{\Sigma}}{\partial \vec{r}} = -\vec{K}^T * M + r^T * M^T * M = 0 \quad (\text{A17})$$

Because  $\vec{r}^{T*}$  is complex valued,  $\frac{\delta \vec{r}^{T*}}{\delta \vec{r}} = 0$ . Thus applying matrix transpose and rearranging the terms of eq. (A17)

$$\begin{aligned} (M^T * M)^T * \vec{r} &= M^T \vec{K} \Rightarrow (M^T M) \vec{r} = M^T * \vec{K} \\ \Rightarrow \vec{r} &= (M^T * M)^{-1} M^T \vec{K} \end{aligned} \tag{A18}$$

Eq (A18) will give us the reflectivity per depth unit and from this we can calculate the impedance.

**Damping constant when calculating reflectivity**

To further understand the inversion we need to discuss how reflectivity per depth unit is computed and the introduction of the matrix M defined in Eq.(A14). However an important aspect must be discussed first. The singularity of the matrix  $M^T * M$  makes it necessary to introduce a damping constant  $\lambda$  when calculating r. This  $\lambda$  is chosen out from the ‘singular value decomposition’ (svd) of the matrix  $M^T * M$ . Now we get an invertible new matrix:

$$L = \text{svd}(M^T * M) \text{ giving } M^T * M + \lambda I$$

I is a unitary matrix of the same order as the matrix  $M^T * M$

$$\begin{aligned} (M^T * M)^T * \vec{r} &= M^T \vec{K} \Rightarrow (M^T M) \vec{r} = M^T * \vec{K} \\ \Rightarrow \vec{r} &= (M^T * M)^{-1} M^T \vec{K} \end{aligned}$$

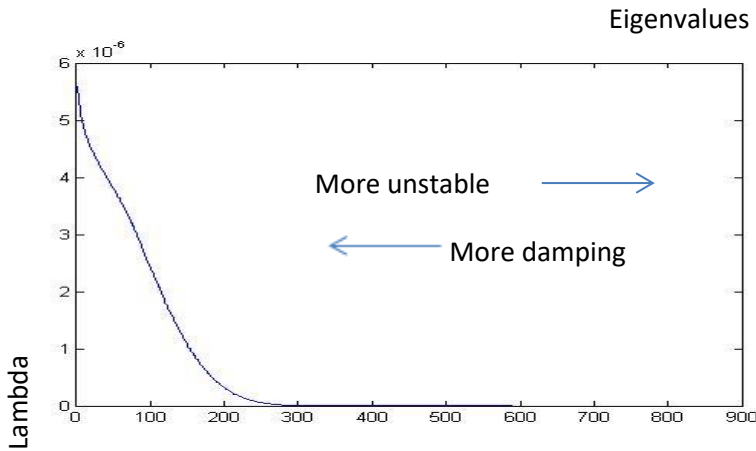


Fig.7 .Damping constant lambda as a function of the eigenvalues of  $M^T * M$

We will choose lambda around (NT/2) eigenvalue of the matrix  $M^T * M$  to be able to use it in the inversion. The output reflectivity (r) will then depend on the value of lambda and introduce damping.

Fig.7 shows that when we choose smaller eigenvalues lambda will increase and r is more damped. When lambda increase we found that the effect of the inversion was less and over a threshold value no effect at all. When we increase eigenvalues, lambda decrease. Then we get less damping but r is also more unstable, and can introduce noise.

It should be taken care to choose the right damping constant ( $\lambda$ ) in order to perform the inversion. The choice must be related to noise level, choice of Butterworth filtering and scaling until one gets a satisfying result. We have not discussed this here, but plan to do it in future research.